

KNOTS IN $\mathbb{R}P^3$

LOUIS H. KAUFFMAN, RAMA MISHRA AND VISAKH NARAYANAN

Abstract: This paper studies knots in three dimensional projective space. Our technique is to associate a virtual link to a link in projective space so that equivalent projective links go to equivalent virtual links (modulo a special flype move). We apply techniques in virtual knot theory to obtain a Jones polynomial for projective links. We show that this is equivalent to the known Jones polynomial defined by Drobotukhina for them. We apply virtual Khovanov homology and the virtual Rasmussen invariant of Dye, Kaestner, and Kauffman to projective links. We compare this cohomology theory with the Khovanov type theory developed by Manolescu and Willis for projective knots. We show that these theories are essentially equivalent.

Mathematics subject classification: 57K10, 57K12, 57K14

1. INTRODUCTION

Our goal is to understand the knot theory of the real projective three space, $\mathbb{R}P^3$. Since $\mathbb{R}P^3$ is a manifold close to S^3 , it is natural to expect that the knot theory in these manifolds are closely related. Virtual knot theory is a perturbation of classical knot theory. We perturb it further, by adding a special move, called the “simple flype” and obtain a virtual model for knots in projective space. Thus structures available in the virtual world can be exported to the projective space, to obtain invariants for projective knots. One of the most interesting problems in projective knot theory, is to detect whether a knot is affine. The property of a projective knot being non-affine is represented by the property of its virtual model being non-classical. Thus, some theorems like Theorem 3, known about non-classical virtual knots can be used to study the non-affineness of projective knots.

We show that the virtual bracket polynomial can be used to construct a bracket polynomial for projective knots. By normalizing this we obtain a Jones type polynomial for projective knots. A version of Jones polynomial for projective knots was defined by Drobotukhina [17] by using the diagrammatic theory obtained by projecting a knot in $\mathbb{R}P^3$ to some projective plane and expanding crossings by the Kauffman skein relation. It turns out that both the polynomials are equivalent.

We construct a Khovanov-type homology theory by using the Khovanov homology for virtual knots defined by Manturov [15]. The Lee deformation and a Rasmussen invariant for this obtained by Dye, Kaestner and Kauffman [2] descends to a Rasmussen invariant for projective knots. Hence we have theorems like Theorem 4, regarding the equality of the 4-ball genus and the Seifert genus of positive knots in $\mathbb{R}P^3$. Manolescu and Willis [14] defined a Khovanov homology and a Rasmussen invariant for projective knots with

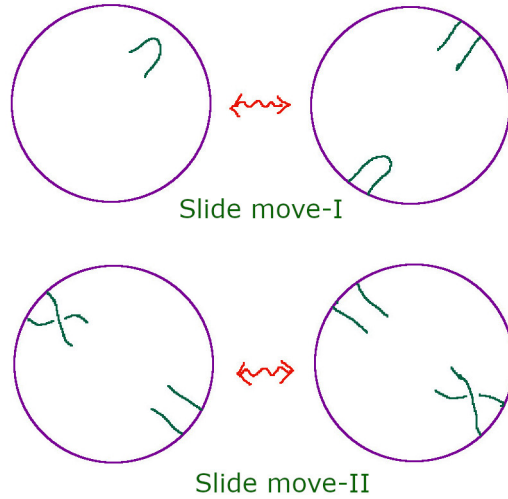


FIGURE 1.

very different methods. They proved a theorem establishing the equivalence of 4-ball genus and the Seifert genus for positive knots. It is natural to wonder how these two cohomology theories are related. We provide a structural comparison between the two and we show that they are both essentially equivalent. Thus most of the known results about projective knots can be seen as coming from this virtual model for them.

Organization of the paper: In Section 2 we introduce the virtual model for projective knots by adding an extra move, called the “flype move” to the equivalence of usual virtual knots. Then we prove that the bracket polynomial for usual virtual knots is invariant under the flype move (Theorem 1). Then a theorem about affine knots is proved as Theorem 2 which results in Corollary 3 which gives an obstruction for a projective knot to be affine. In Section 3 we provide some examples showing the application of Corollary 3. Section 4 and Section 5 provide some details about virtual knot theory which will be used extensively in the later parts of the paper. Section 6 defines the Khovanov-type invariant for projective knots. Theorem 4 is proven for projective knots. Then in 6.1 we compare our theory with that of [14] and show that they are equivalent. In Section 7 we discuss some properties of projective knots, which our virtual model cannot capture. We add an Appendix as Section 8, which includes the *Mathematica* code for bracket calculation of a 13 crossing knot appearing in Section 6.

2. KNOTS IN PROJECTIVE SPACE, VIRTUAL KNOTS AND THE BRACKET POLYNOMIAL

Knots in projective space RP^3 can be represented by diagrams in RP^2 where the projective plane RP^2 is represented by a disk with antipodal identifications on the boundary. Moves on these diagrams consist in the Reidemeister moves plus two slide moves across the boundary identification as shown in Figure 1.

In this figure note that when a crossing slides across the boundary its oriented sign remains the same. We are viewing the projection of the diagram to the projective plane in



FIGURE 2. Sliding a crossing over a half twist

terms of the embedding of a thickened projective plane in $RP^2 \subset RP^3$. The neighbourhood of the projective plane in the projective three space is a twisted I -bundle over the projective plane. One can visualize the slide move by imagining sliding a diagram drawn on a Möbius strip through the twist in the strip. Because we respect the twisted I -bundle, the viewer of the diagram twists as he/she moves through the twist. This means that the crossing sign is retained as shown in Figure 2.

Since the Reidemeister and slide moves are compatible with crossing types as we have discussed above, one can define the bracket polynomial expansion and its writhe normalization just as we have done in the case of diagrams in the plane or on the two dimensional sphere. This means that the loop counting for the bracket polynomial can be done by representing the knot in projective space by a tangle drawn in the projective disk and identifying the endpoints of this tangle according to the antipodal identifications on the boundary of the disk. This identification can be simplified by noting that for n -strands in the tangle (top and bottom) there is a canonical permutation corresponding to the antipodal map. The tangle may not have the same number of endpoints at the top and bottom in which case we can still use the antipodal identification.

We define a mapping π from diagrams in the projective plane to virtual knot and link diagrams. See Figure 3. Diagrammatically the association of a virtual link diagram to a tangle representation of a projective knot is this: Regard the disk for the projective tangle as embedded in the plane or two-sphere. Draw the connecting arcs between identified points on the boundary of the disk as actual arcs embedded in the complement of the disk in the plane. The arcs may cross transversally and these crossings are taken as virtual crossings. If T is the tangle associated with the projective link, let $\pi(T)$ denote the corresponding virtual link diagram we have just described. We will now prove that if K and L are equivalent projective links, then $\pi(K)$ and $\pi(L)$ are related by a simple set of moves on virtual links. Thus certain invariants of virtual links can be used to construct projective link invariants. In the case of the bracket polynomial we shall show that $\langle K \rangle = \langle \pi(K) \rangle$ for any projective link K where the first bracket is the bracket as defined directly on the projective diagram and the second bracket is the usual simplest bracket

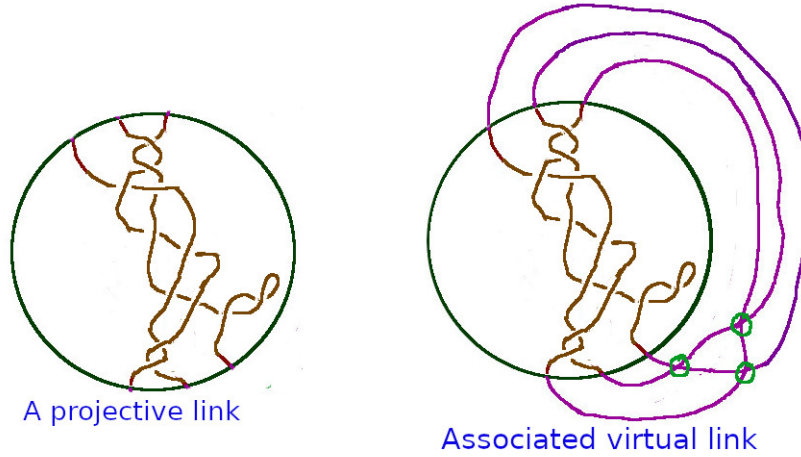


FIGURE 3. Association of a virtual link to a projective link.



FIGURE 4. Flype move

polynomial for virtual links.

By using this mapping of projective links to virtual links, we can apply invariants of virtual links to measure properties of links in projective space. We will give a number of examples of this correspondence in the course of the paper.

The scheme described above will associate a diagram of a virtual link with the diagram of a projective link. Now we study this association in more detail. It is easy to see that, if we perform a slide move by transferring a crossing across the projective plane at infinity, the associated virtual link before and after are related by the move shown in Figure 4. We call this as the “Flype move”. We prove the following.

Proposition 1. *Any two virtual link diagrams associated with a link in $\mathbb{R}P^3$, are related by a sequence of ordinary virtual Reidemeister moves [7] and the Flype move.*

Let L and L' be projective links that are equivalent in $\mathbb{R}P^3$. Let $\pi(L)$ and $\pi(L')$ be the associated virtual links. Then $\pi(L)$ and $\pi(L')$ are related by a sequence of standard virtual moves and the Flype move.

Proof: The virtual link diagrams associated to the diagrams of a projective link before and after performing any Reidemeister move on a projective link diagram is clearly related by the corresponding generalized Reidemeister move on virtual link diagrams. Hence it is enough to examine how the associated virtual links are related before and after performing each of the slide moves shown in Figure 1. It is clear the virtual link diagrams associated before and after performing a slide move-I are related by a virtual Reidemeister move-I. Similarly, the virtual link diagrams associated before and after a Slide move-II are related by a Flype move. Since any two diagrams of a projective link are related by a finite sequence of Reidemeister moves and slide moves [17], the proposition follows. \square

Let PVK denote the set of virtual links up to usual Reidemeister moves and the Flype move. Then by Proposition 1, we have that, the association defined above will induce a mapping,

$$\pi : \{Links\ in\ projective\ space/ambient\ isotopy\} \rightarrow PVK.$$

Corollary 1. *If K is an affine link in $\mathbb{R}P^3$, then $\pi(K)$ is a classical virtual knot.*

Corollary 2. *Any invariant of virtual link diagrams which invariant under the flype move is an invariant of links in $\mathbb{R}P^3$.*

We have elsewhere called the equivalence relation of virtual links generated by standard moves and the Flype move, Z-Equivalence. Thus projective links that are equivalent in $\mathbb{R}P^3$ map to Z-equivalent virtual links.

Theorem 1. *The normalized Kauffman bracket polynomial is invariant under the flype move.*

Proof: Refer to Figure 5. \square

Thus we may use the Kauffman bracket polynomial on virtual links to construct invariants of links in $\mathbb{R}P^3$. Consider the normalized bracket polynomial on virtual knot diagrams defined by setting $B = A^{-1}$ and normalizing by dividing with the loop value $-A^2 - A^{-2}$. The normalized bracket of a virtual link with writhe $w(K)$ is given by the formula,

$$f_K(A) = \frac{1}{-A^{3w(K)}(-A^2 - A^{-2})} \langle K \rangle,$$

a Laurent polynomial of the variable A . When we change variables from A to t by the rule, $A = t^{-\frac{1}{4}}$ we get a Laurent polynomial in variable t . This is the Jones polynomial. In this paper we call f_K the normalized bracket polynomial, as the function of the variable A .

Now for a knot K in $\mathbb{R}P^3$, if $\pi(K)$ is any virtual link associated to K using a diagram as described above, we define,

$$f_K := f_{\pi(K)}.$$

Notice that by Theorem 1, f_K is well defined. In what follows we will use this notation quite frequently. The following theorem is from [17].

$$\begin{aligned}
& \langle \text{Diagram 1} \rangle = A \langle \text{Diagram 2} \rangle + B \langle \text{Diagram 3} \rangle \\
& = A \langle \text{Diagram 4} \rangle + B \langle \text{Diagram 5} \rangle \\
& = A \langle \text{Diagram 6} \rangle + B \langle \text{Diagram 7} \rangle \\
& = \langle \text{Diagram 8} \rangle
\end{aligned}$$

FIGURE 5. Invariance of the bracket polynomial under the flype move.

Theorem 2. *If K is an affine knot in $\mathbb{R}P^3$, then the degree of each monomial in f_K is an integer multiple of 4.*

Proof: Note that if J is a classical knot then the degree of each monomial in f_J is an integer multiple of 4. Since K is an affine knot it has a diagram such that the associated tangle T has no boundary points. Hence there are no virtual crossings in $\pi(T)$. Let J be a classical knot obtained by removing a projective plane disjoint from K . Notice that $f_K := f_{\pi(T)} = f_J$. Hence all the monomials in f_K have degree as integer multiples of 4.

Corollary 3. *If K is a knot in $\mathbb{R}P^3$ and f_K has a monomial with degree not divisible by 4, then K is non-affine.*

3. EXAMPLES

Let J be the projective knot shown in the left of Figure 6. It is clearly a class-0 non-affine knot since it is covered in S^3 by a link with two components and which has linking number 2 between its components. The virtual knot shown on the right of Figure 6 is constructed using the same method as above. Using this virtual knot one can easily calculate,

$$f_J = -A^{-4} - A^{-6} + A^{-10}.$$

Hence the normalized bracket polynomial detects that J is non-affine, since two of the exponents are not divisible by 4.

Let K_1 be the knot shown in Figure 7. We have,

$$f_{K_1} = 3 + A^{-8} - 2A^{-4} - 2A^4 + 2A^8 - 2A^{12} + A^{16}$$

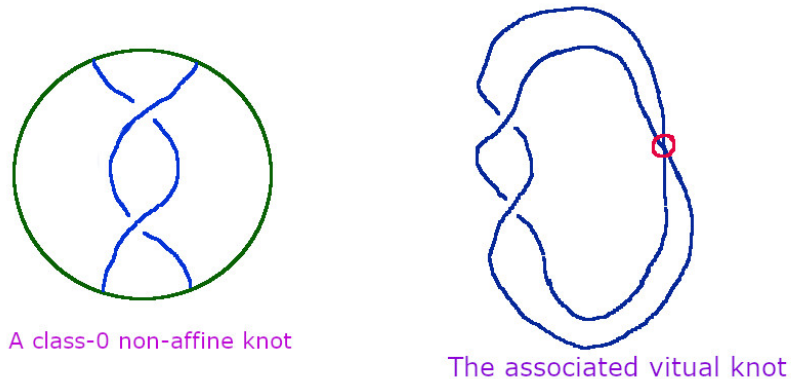


FIGURE 6. The virtual knot associated with a class-0 knot.

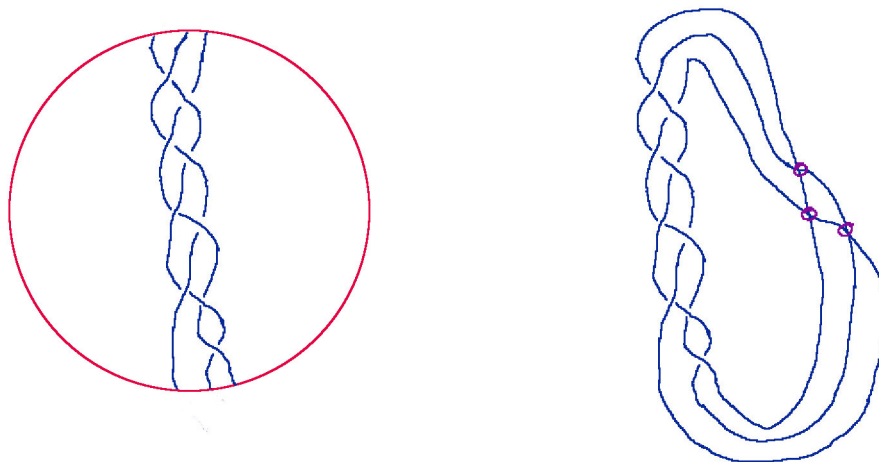


FIGURE 7. The virtual link associated to a class-1 knot.

Since the knot is class-1, it is non-affine, although the bracket does not detect it. It is noteworthy that the bracket detects the chirality of K_1 .

Let W_1 be the virtual knot shown in Figure 8. It is a virtual knot associated to a link K_2 that is the projective closure of the W-tangle [18].

$$f_{W_1} = -A^{-8} - A^{-4}$$

Thus W_1 has the normalized bracket of a classical knot.

Now let W_2 be the virtual link shown in Figure 9. It is the virtual link associated to a component of the link K_2 , which we call K_3 .

$$f_{W_2} = A^{-14}(1 - 2A^4 + 2A^8 + A^{10} - 2A^{12} - A^{14} + A^{16} + A^{18})$$

Thus K_3 is non-affine by Corollary 3. Since K_3 is a component of K_2 , K_2 is non-affine.

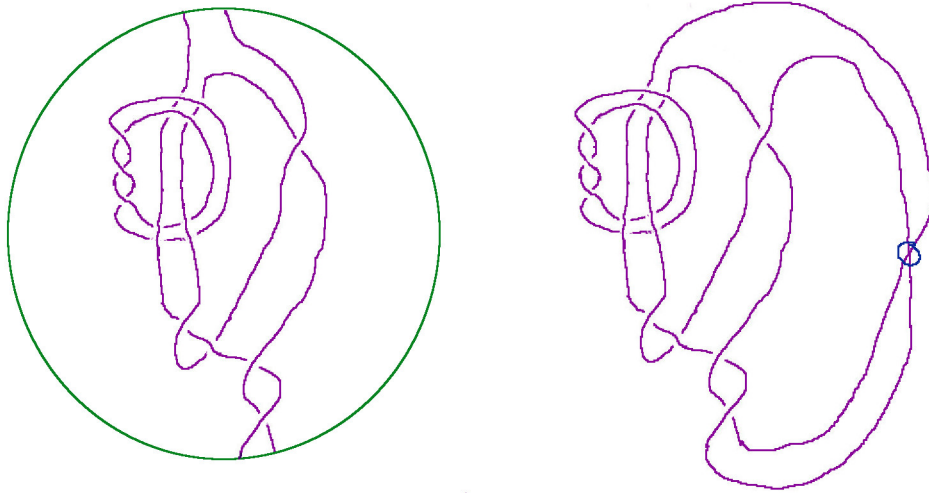


FIGURE 8. The virtual link associated to the projective W-tangle.

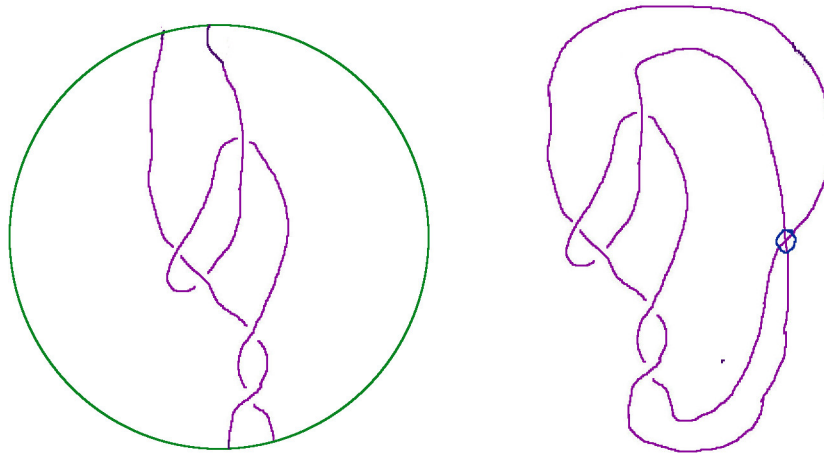


FIGURE 9. A component of the virtual link in Figure 8.

4. VIRTUAL KNOT THEORY

Knot theory studies the embeddings of curves in three-dimensional space. Virtual knot theory studies the embeddings of curves in thickened surfaces of arbitrary genus, up to the addition and removal of empty handles from the surface. Virtual knots have a special diagrammatic theory, described below, that makes handling them very similar to the handling of classical knot diagrams. Many structures in classical knot theory generalize to the virtual domain.

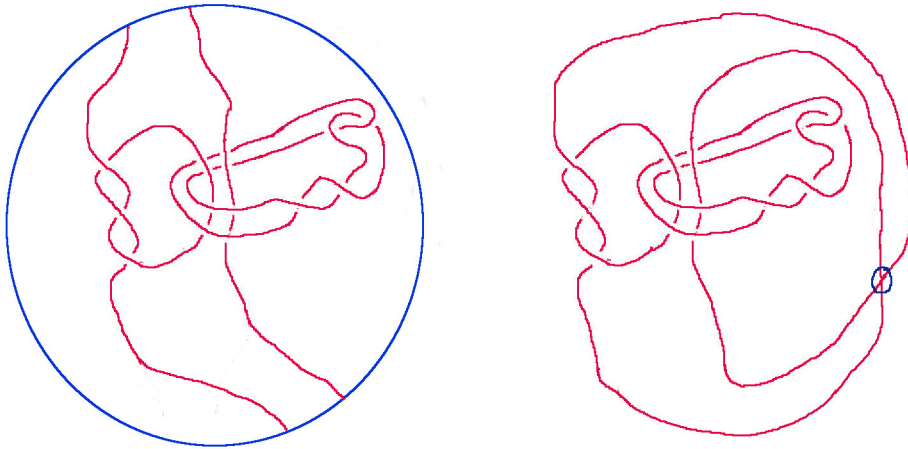


FIGURE 10. The virtual link associated to a projective Thistlethwaite tangle.

In the diagrammatic theory of virtual knots one adds a *virtual crossing* (see Figure 11 that is neither an over-crossing nor an under-crossing. A virtual crossing is represented by two crossing segments with a small circle placed around the crossing point.

Moves on virtual diagrams generalize the Reidemeister moves for classical knot and link diagrams. See Figure 11. One can summarize the moves on virtual diagrams by saying that the classical crossings interact with one another according to the usual Reidemeister moves while virtual crossings are artifacts of the attempt to draw the virtual structure in the plane. A segment of diagram consisting of a sequence of consecutive virtual crossings can be excised and a new connection made between the resulting free ends. If the new connecting segment intersects the remaining diagram (transversally) then each new intersection is taken to be virtual. Such an excision and reconnection is called a *detour move*. Adding the global detour move to the Reidemeister moves completes the description of moves on virtual diagrams. In Figure 11 we illustrate a set of local moves involving virtual crossings. The global detour move is a consequence of moves (B) and (C) in Figure 11. The detour move is illustrated in Figure 12. Virtual knot and link diagrams that can be connected by a finite sequence of these moves are said to be *equivalent* or *virtually isotopic*.

Another way to understand virtual diagrams is to regard them as representatives for oriented Gauss codes [4], [8, 9] (Gauss diagrams). Such codes do not always have planar realizations. An attempt to embed such a code in the plane leads to the production of the virtual crossings. The detour move makes the particular choice of virtual crossings irrelevant. *Virtual isotopy is the same as the equivalence relation generated on the collection of oriented Gauss codes by abstract Reidemeister moves on these codes.*

Figure 13 illustrates the two *forbidden moves*. Neither of these follows from Reidemeister moves plus detour move, and indeed it is not hard to construct examples of virtual knots that are non-trivial, but will become unknotted on the application of one or both of the

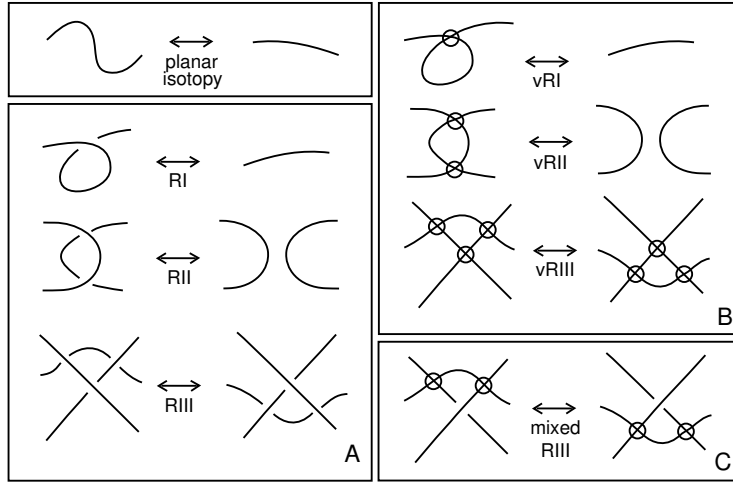


FIGURE 11. Moves

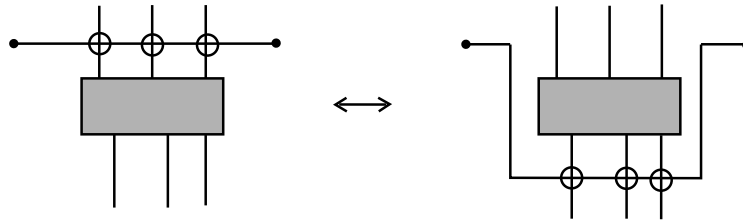


FIGURE 12. Detour Move

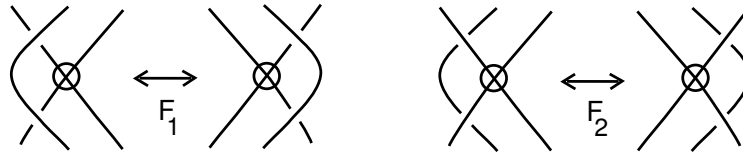


FIGURE 13. Forbidden Moves

forbidden moves. The forbidden moves change the structure of the Gauss code and, if desired, must be considered separately from the virtual knot theory proper.

5. INTERPRETATION OF VIRTUALS LINKS AS STABLE CLASSES OF LINKS IN THICKENED SURFACES

There is a useful topological interpretation [8, 10] for this virtual theory in terms of embeddings of links in thickened surfaces. Regard each virtual crossing as a shorthand for a detour of one of the arcs in the crossing through a 1-handle that has been attached to the 2-sphere of the original diagram. By interpreting each virtual crossing in this way, we obtain an embedding of a collection of circles into a thickened surface $S_g \times R$ where g is

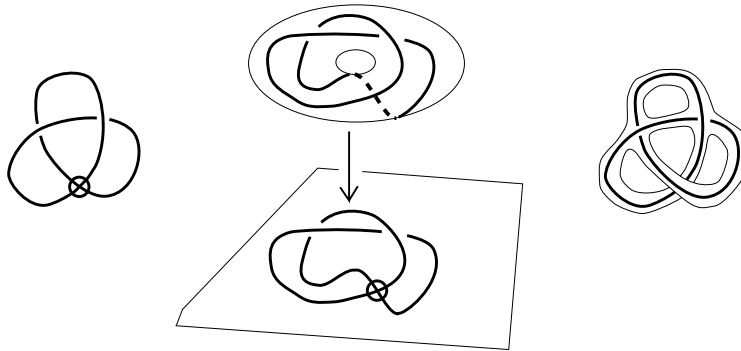


FIGURE 14. Surfaces and Virtuals

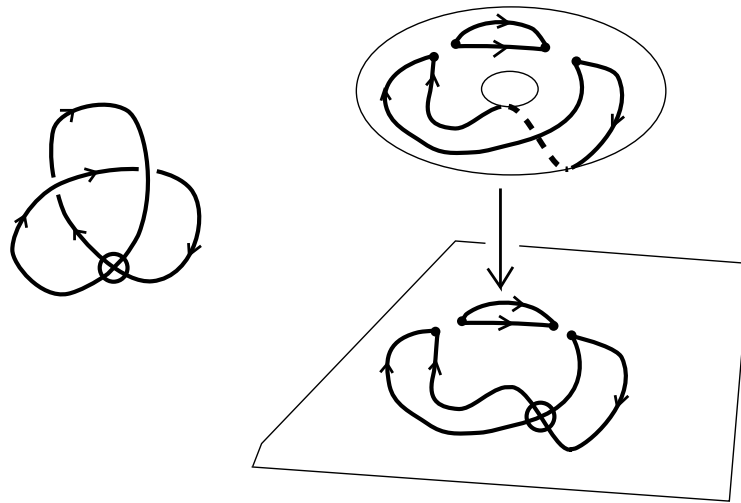


FIGURE 15. Surfaces and Virtual States

the number of virtual crossings in the original diagram L , S_g is a compact oriented surface of genus g and R denotes the real line. We say that two such surface embeddings are *stably equivalent* if one can be obtained from another by isotopy in the thickened surfaces, homeomorphisms of the surfaces and the addition or subtraction of empty handles (i.e. the knot does not go through the handle).

We have,

Theorem 1 [8, 11, 10, 1]. *Two virtual link diagrams are isotopic if and only if their corresponding surface embeddings are stably equivalent.*

In Figure 14 and Figure 15 we illustrate some points about this association of virtual diagrams and knot and link diagrams on surfaces. Note the projection of the knot diagram on the torus to a diagram in the plane (in the center of the figure) has a virtual crossing in the planar diagram where two arcs that do not form a crossing in the thickened surface project to the same point in the plane. In this way, virtual crossings can be regarded

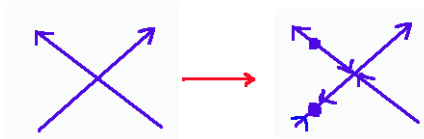


FIGURE 16. An oriented crossing and the corresponding source-sink orientation.

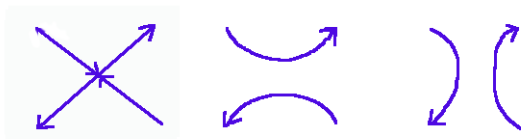


FIGURE 17. The orientations induced on the resolved arcs.

as artifacts of projection. The same figure shows a virtual diagram on the left and an “abstract knot diagram” [12, 1] on the right. The abstract knot diagram is a realization of the knot on the left in a thickened surface with boundary and it is obtained by making a neighborhood of the virtual diagram that resolves the virtual crossing into arcs that travel on separate bands. The virtual crossing appears as an artifact of the projection of this surface to the plane. The reader will find more information about this correspondence [8, 11] in other papers by the author and in the literature of virtual knot theory.

6. KHOVANOV AND RASMUSSEN INVARIANTS OF KNOTS IN PROJECTIVE SPACE

Dye, Kaestner and Kauffman in [2], have discussed the structure of Khovanov Homology as defined by Manturov [15] for virtual knots and links and they have extended this structure to a version of Lee Homology and defined a Rasmussen invariant for virtual knots and links. We can use our mapping,

$$\pi : \{\text{Links in projective space/ambient isotopy}\} \rightarrow PVK$$

constructed in Section 2, from projective links to virtual links to define Khovanov homology and a Rasmussen invariant for projective links by taking, for a projective link K , the Khovanov homology of $\pi(K)$ and the Rasmussen invariant of $\pi(K)$.

We now will give a brief discription of the homology theory. Given a diagram of a projective knot K , we may construct the diagram for $\pi(K)$. Then by giving an arbitrary numbering to the crossings, of $\pi(K)$ except the virtual crossings, we can obtain the cube of resolutions. We take the convention, that all A states are arranged first and all B states come at last. That is, each edge corresponds to a crossing switching its A smoothing to a B smoothing. Each resolution consists of a collection of unknotted circles possibly with virtual crossings. To each such circle, we associate a rational vector space V of dimension two, with an abstract basis $\{1, X\}$. This vector space is a turned into a Frobenius algebra by the multiplication m , comultiplication Δ , unit map ν and counit map ϵ . These are

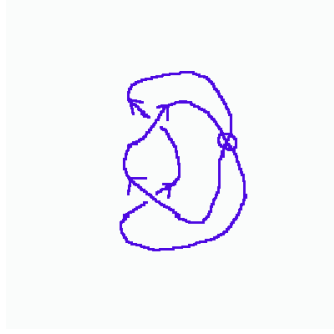


FIGURE 18. An oriented virtual diagram of an affine unknot.

defined as follows,

$$m : V \otimes V \rightarrow V;$$

$$m(1 \otimes 1) = 1;$$

$$m(1 \otimes x) = m(x \otimes 1) = x;$$

$$m(x \otimes x) = 0$$

$$\Delta : V \rightarrow V \otimes V;$$

$$\Delta(1) = 1 \otimes x + x \otimes 1;$$

$$\Delta(x) = x \otimes x$$

$$\nu : \mathbb{Q} \rightarrow V;$$

$$\nu(1) = 1$$

$$\epsilon : V \rightarrow \mathbb{Q};$$

$$\epsilon(1) = 1;$$

$$\epsilon(x) = 0$$

To every vertex of the cube, which is a state consisting of several state circles, we associate a module which is the tensor product of n number of copies of V , where n is the number of state circles. For each edge which represents the change of the some crossing switching from A smoothing to a B smoothing, we associate one of the three possible maps between the modules on its vertices. If it is a $2 - 1$ bifurcation we use m , if its is a $1 - 2$ bifurcation we use Δ and if it is a $1 - 1$ bifurcation, we use the zero map denoted by η .

In the classical case, none of the edges of the cube will correspond to a 1-1 bifurcation and the only maps appearing on the edges are m and Δ 's. The signs assigned to these maps by using the ordering of crossings makes the squares anti-commute. Thus we get a cochain complex and a cohomology theory.

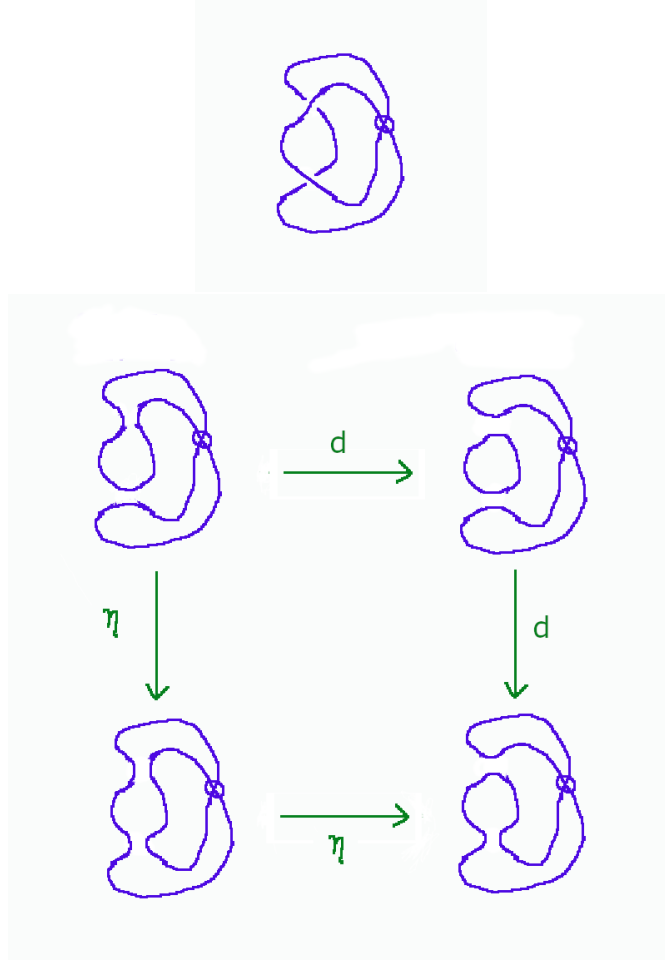


FIGURE 19. An example of a 1-1 bifurcation. On the one hand $\eta \circ \eta = 0$, so to make $d \circ d = 0$ on the other side, there should be signs.

In a general projective knot K , the diagram of $\pi(K)$ may have virtual crossings. Thus it is possible to have a 1 – 1 bifurcations on some edges as in the example shown in Figure 18, for which the cube is shown in Figure 19. To make all the squares commute, we will use the method of Manturov [15] which is re-interpreted by Dye, Kaestner and Kauffman [2]. The basic idea is as follows.

Given a knot diagram, we choose an arbitrary orientation on it. See Figure 18. This induces an orientation at each crossing. At each crossing, we give a “source-sink” orientation corresponding to the induced local orientation by the scheme shown in Figure 16. The dots on the arcs, are called “cut points”, which denote the mismatch of the orientations on both sides. The source-sink orientations on crossings will induce orientations on the resolved arcs as in Figure 17. Hence in every state circle we may get multiple arcs with different orientations separated by cut points. We will mark a base point on one of these arcs on every circle. Refer to Figure 21. The orientation at the base point on every

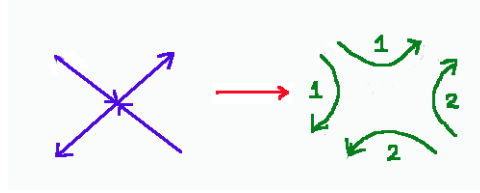


FIGURE 20. The prescription for ordering the arcs of states.

state circle is chosen as a global orientation for that circle.

Now an arbitrary numbering is chosen on the state circles of each state. As a smoothing is bifurcating, the numbering on the states before and after can be compared. At the states before and after, a permutation of the circles where the circles involved in the bifurcation is promoted to the first position is considered according to the conventions indicated in Figure 20. The signs of these permutations at each ends are added to the algebra elements on both ends of the differential.

Every time an algebra element passes through a cut point, it gets “barred”. Notice that, to bar and element in the Frobenius algebra, means if it is an X we multiply it with -1 , if it is 1 then we leave it as it is and extend these operations linearly to a general element in the algebra. That is, $\forall a, b \in \mathbb{Q}$, we define:

$$\overline{a1 + bX} = a1 - bX.$$

The algebra element on a state circle should be thought of as placed at the base point. Whenever the differential is applied the algebra elements at the base point(s) before is transported to the site, and the newly produced elements at the site will be transported to the new base point(s). The transports are always in the direction decided by the orientation of each of the state circles. direction of the global orientation on each circle. Before applying the differential, we bar the elements of the algebra on every circle p times, where p is the number of cutpoints it passes through while reaching the site from the base point before the bifurcation. Similarly the newly produced algebra elements will get barred on the path from the concerned site to the base point each time it passes a cut point. And for the algebra elements on the circles, which are not taking part in the bifurcation, they will be transported to the new base point after bifurcation from the initial base point and barred accordingly.

With this sign convention and the standard conventions in classic Khovanov homology, d becomes a differential. That is, $d \circ d = 0$ and we have a graded cohomology theory for all the $\pi(K)$. As shown in Section 1, since the Kauffman bracket polynomial is invariant under the flype move (refer to Figure 5), it follows that this is independent of the diagram chosen for the projective knot K . Thus, the cohomology groups only depend on K . We will denote this as $Kh(K)$.

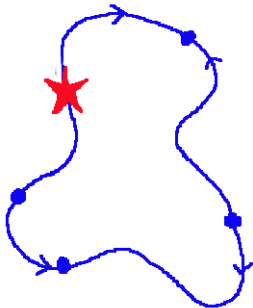


FIGURE 21. A typical state circle. The star denotes a base point. The orientation of this arc will be chosen as the direction in which the elements in the algebra flows through this state circle.

In order to obtain a result about projective links from this result, we need to discuss cobordism of projective links and how it is related to corresponding cobordisms of the virtual links in the image of the mapping P . This notion of cobordism can be explained combinatorially at the diagram level. We say that two projective link diagrams are *cobordant* if one can be obtained from the other by a sequence of oriented saddle replacements, births and deaths of circles and isotopy of projective links. See Figure 22. The result of such a sequence of changes in the diagram can be regarded formally as the generation of an orientable surface whose boundary consists in the first and second diagrams. If diagrams K and K' are cobordant, then the genus of the cobordism surface is called the genus of the cobordism between K and K' . These notions apply to classical diagrams, to diagrams of links in RP^2 that represent projective links in RP^3 , and to virtual link diagrams. In the classical and virtual cases, every link is cobordant to the empty link. That is, for a given diagram K there is a sequence of saddles, births and deaths that results in an empty diagram. Correspondingly, there is a surface whose boundary is the link K . In the projective case, this is true only for null homologous links. In the case of a class-1 link we can always construct a cobordism to an unknotted loop that represents a projective line in RP^2 diagrammatically the class-1 unknot in RP^3 in terms of the corresponding embedding in the three dimensional projective space. We call these surfaces the *4-ball surfaces for K* uniformly where this terminology does in fact indicate a surface in the four-ball in the classical case. We call the least possible genus among all such surfaces the *4-ball genus* $g_4(K)$.

In Figure 22 we illustrate cobordism of diagrams under saddle points, births and deaths. In Figure 23 we illustrate the construction of the Seifert surface for a classical trefoil knot. In Figure 24 we show how the Seifert construction can be seen as cobordism by performing saddle points near each crossing. In Figure 25 we show how this cobordism analogue for the Seifert construction can be used to produce a virtual Seifert surface for a virtual knot.

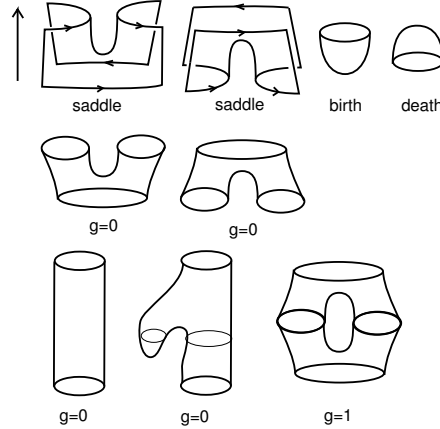


FIGURE 22. Cobordism of Diagrams

The main theorem of [2] on virtual knot cobordism using Khovanov homology for virtuals is,

Theorem 3. *The virtual 4-ball genus of a positive virtual link L is equal to its virtual Seifert genus. The virtual Seifert genus has the specific formula $g = \frac{(C+1-S)}{2}$ where C is the number of classical crossings in L and S is the number of Seifert circuits, obtained by smoothing all the crossings in an oriented fashion.*

Theorem 4. *The 4-ball genus of a positive projective knot is equal to its Seifert genus.*

Proof: From a link K in RP^3 by applying our mapping P we obtain a virtual link $\pi(K)$. It is then the case that if K and K' are cobordant projective links, then $\pi(K)$ and $\pi(K')$ are cobordant virtual links. K is positive if and only if $\pi(K)$ is positive. Hence the theorem follows from applying Theorem 3. \square

If K is a projective link which has an odd number of class-1 components (a class-1 link) then the most general cobordism will always take K to a class-1 unknot. Call this α . Then $\pi(\alpha)$ is an unknotted virtual loop and so bounds a disk. This means that cobordisms of class-1 projective links differ from the cobordisms we can apply to their virtual counterparts. But we can define the genus of a class-1 link K to be the minimal genus of a surface that is a cobordism of K to α . Since $\pi(\alpha)$ bounds a disk in the virtual context, we see that, $g_4(\pi(K))$ is equal to this minimal genus for K in projective space.

For a positive non-affine knot K that is not class-1 projective space, the Theorem 4 applies to give $g_4(K)$ as a projective knot. For example, view Figure 26 where we illustrate such a knot in the lower portion of the figure and determine that $g = g_4(K) = 1$ by finding that the virtual version of K has $C = 2, S = 1$ and applying the formula $g = \frac{(C+1-S)}{2} = \frac{(2+1-1)}{2} = 1$.

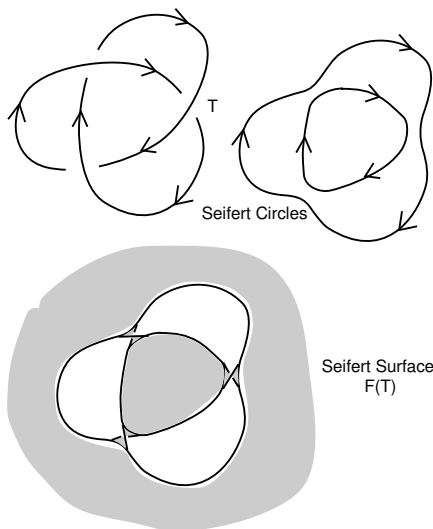
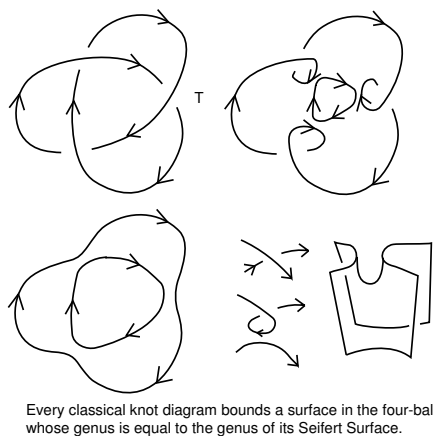


FIGURE 23. Classical Seifert Surface



Every classical knot diagram bounds a surface in the four-ball whose genus is equal to the genus of its Seifert Surface.

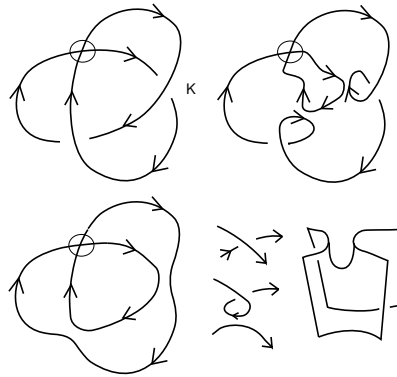
FIGURE 24. Virtual Cobordism Surface

It is to be noted that this formula works only for positive knots. The knot R shown in Figure 27, has the following Jones polynomial,

$$f_R = 2 + A^{-18} + A^{-16} - A^{-14} - 2A^{-12} + 2A^{-8} - 2A^{-4} - A^{-2} + A^2,$$

which has monomials with degree not congruent to 4. Hence by Corollary 3 it is non-affine. See the appendix for the calculation of bracket polynomial. R is a slice, since it is ribbon and hence it will have 4-ball genus 1. But $\frac{C+1-S}{2} = \frac{13+1-6}{2} = 4$.

Ciprian Manolescu and Michael Willis defined Khovanov Homology and a Rasmussen invariant [14] by modifying a Khovanov homology theory for projective knots defined by Bostjan Gabrovsek [3]. Their definitions are not the same as ours, but they obtain very similar results about positive links. A comparison of the two approaches is called for and we will discuss this comparison below and translate between the two points of view.



Seifert Circle(s) for K

Every virtual diagram K bounds a virtual orientable surface of genus $g = (1/2)(-r + n + 1)$ where r is the number of Seifert circles, and n is the number of classical crossings in K. This virtual surface is the cobordism Seifert surface when K is classical.

FIGURE 25. Virtual Seifert Surface

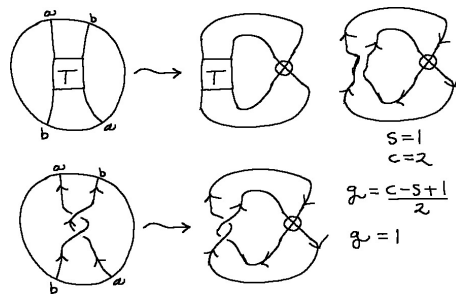


FIGURE 26. Finding Projective Genus

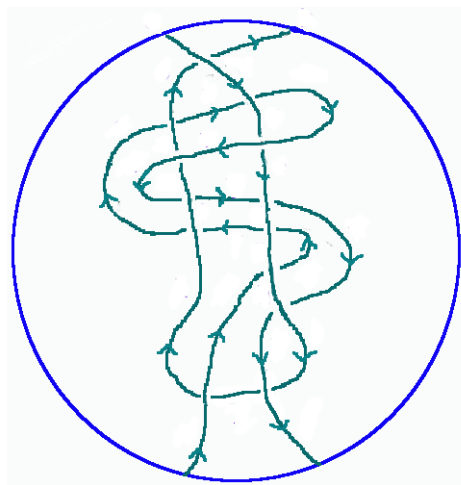


FIGURE 27. A projective ribbon knot with $\frac{C+1-S}{2} = \frac{13+1-6}{2} = 4$.

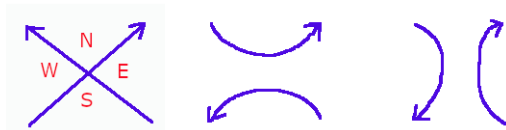


FIGURE 28. Locally consistent orientations given by the cardinal directions.

6.1. **A comparison with [14].** For brevity of notation, in what follows, we will denote the cohomology theory of Dye, Kaestner and Kauffman as DKK theory and the cohomology theory of Manolescu and Willis as the MW theory.

In the MW-theory, they introduce a new Frobenius algebra for the class-1 circles in a state, generated by 1 and \overline{X} , which is isomorphic to the Frobenius algebra above generated by 1 and X . A word of caution is to be mentioned that the \overline{X} in MW theory and the \overline{X} above obtained from barring operation from DKK theory are entirely different. In MW theory, the introduction of this new algebra means that the final Khovanov cohomology has knowledge of the singular homology class represented by the link.

In the MW theory, one has to choose a global orientation on the link diagram and then arbitrary local orientations at each of the crossings. Each of the state circles are given a numbering and global orientation arbitrarily. The chosen local orientations at a crossing determine cardinal directions on the local quarter planes as shown in Figure 28. The cardinal directions at every crossing determines a set of “consistent” orientations on the resolved arcs as in Figure 28. There are three rules for deciding signs, while applying the differential. These are called *Permutation rule*, *Nearby consistency rule* and the *Far orientations rule*.

Permutation rule is exactly same as the rule in the DKK theory, described above, using Figure 20. Nearby consistency rule says that if the consistent orientation on an arc at a newly produced site (see Figure 28), mismatches with the global orientation then this determines a sign on the X component of the algebra element produced there. Comparing Figures 17 and 28, it is clear the local orientations on the state circles are exactly the same in both the theories. Hence a state in the DKK theory may be used to construct a state in the MW theory if we change a source-sink orientation to a cardinal orientation and vice-versa, as shown in Figure 29.

We can use the DKK cutpoint assignment to choose global orientations for each loop in a state. We do this by taking the local orientation at the base point of a circle in a DKK state and then using its direction co-determine a global orientation for the corresponding loop in the MW state. When the differential is applied, the local orientation at the arcs at the site of a loop will be either the same or different from the global orientations according to the parity of number of cutpoints that one must traverse while travelling towards the base point. Now notice that we have chosen to orient the MW state (each loop given an

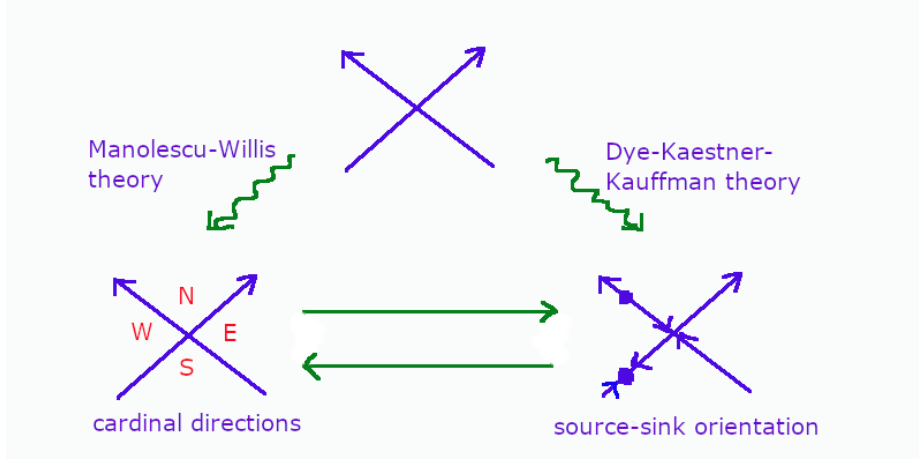


FIGURE 29. Equivalence of our theory with MW theory

orientation) using the local orientations at the basepoint from the DKK state. When the local orientation at a site mismatches with the global orientation, this corresponds to a sign change for the X 's on the MW state by nearby consistency rule. This can occur only when there are odd number of cut points between the base point and the site. Thus the DKK rule involving parity of number of cut points becomes the exact sign change of MW.

The far orientations rule is as follows. After applying the differential, the result is multiplied with a sign corresponding to the parity of the number of circles, which do not pass through the neighbourhood of the bifurcating crossing and are carrying an X and have distinct orientations in the diagrams before and after the bifurcation. Note that the orientations of a far circle flips when the base points chosen before and after are separated by an odd number of cutpoints. Which means, in the new state, the algebra element on that circle has to be barred in the DKK rule. Hence this rule is already implied by the cutpoint rules.

Thus, in this special set of MW states determined by DKK states, the signs sprinkled by either of the two theories are coherent. So we have an equivalence of the two cohomology theories. Given a projective link diagram L , we have natural chain map,

$$\alpha : C_{DKK}(L) \longrightarrow C_{MW}(L)$$

where $C_{DKK}(L)$ represents the chain complex associated as above and $C_{MW}(L)$ is chain complex associated as in [14], with \bar{X} replaced by X . From the discussion above, we have the following theorem.

Theorem 5. *The chain map α induces isomorphisms on the cohomology groups.*

Remark 1. *Our cohomology theory can be modified by adding markings for class-1 state circles so that we get cohomology groups that are identical to those in the MW theory.*

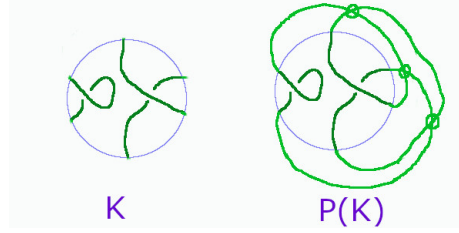


FIGURE 30. A projective knot and the corresponding virtual knot.

In our method, we apply the map π to a projective knot diagram, drawn on a disk to obtain a virtual diagram, and then construct the cube of resolutions for it. Instead of this, we can first construct the cube of resolutions of a projective diagram on the disk where the states will consist of diagrams of disjoint unknots and then apply the map π to each of the vertices and obtain the cube of resolutions of the corresponding virtual knot. Note that out of in every state, most of the state circles are class-0 unknots. There can be at most one class-1 unknot in a state. This will be represented by an arc which connects some pair of diametrically opposite points. Before applying the map π , we may mark this state circle, by putting a diamond on the arc. Now after applying the map π , in the cube of resolutions of the virtual knot, we have a unique state circle, in those states with the marking. While applying the TQFT, these circles are mapped to a different Frobenius algebra V^* , generated by $1^*, x^*$. The structure maps for this algebra are as follows.

$$\begin{aligned}
 m : V \otimes V &\rightarrow V; \\
 m(1^* \otimes 1^*) &= 1^*; \\
 m(1^* \otimes x^*) &= m(x^* \otimes 1^*) = x^*; \\
 m(x^* \otimes x^*) &= 0
 \end{aligned}$$

$$\begin{aligned}
 \Delta : V &\rightarrow V \otimes V; \\
 \Delta(1^*) &= 1^* \otimes x^* + x^* \otimes 1^*; \\
 \Delta(x^*) &= x^* \otimes x^*
 \end{aligned}$$

$$\begin{aligned}
 \nu : \mathbb{Q} &\rightarrow V; \\
 \nu(1^*) &= 1^*
 \end{aligned}$$

$$\begin{aligned}
 \epsilon : V &\rightarrow \mathbb{Q}; \\
 \epsilon(1^*) &= 1^*; \\
 \epsilon(x^*) &= 0
 \end{aligned}$$

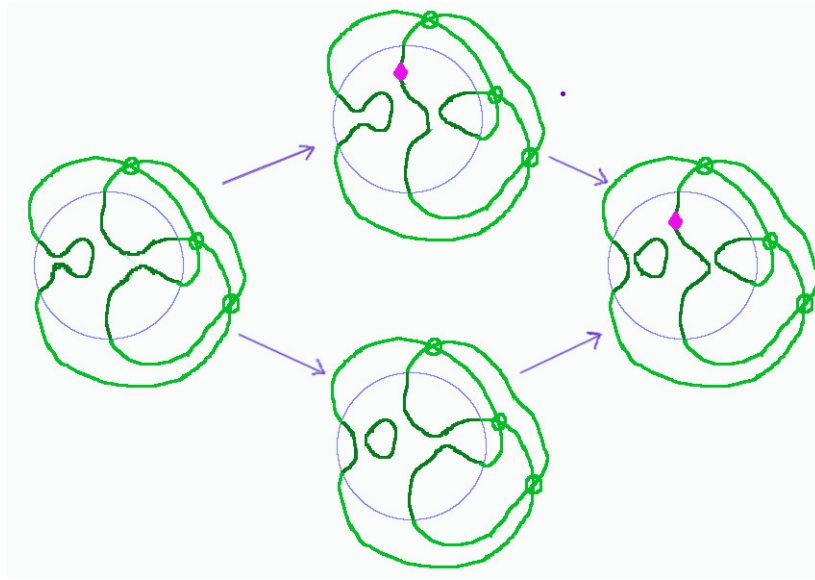


FIGURE 31. The cube of resolutions for a projective virtual knot. The class-1 state circles are marked with a diamond.

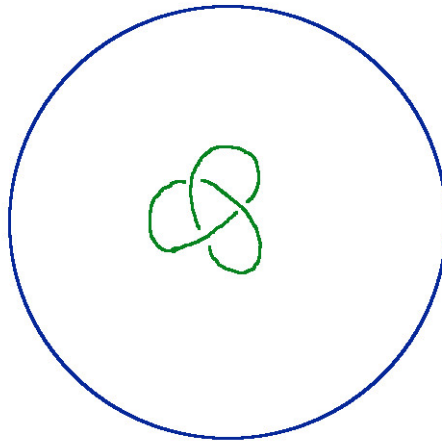


FIGURE 32. Affine trefoil knot

7. WHAT THIS METHOD CANNOT SEE!

The association of a virtual knot to a projective knot in this way indeed is not a complete solution to the problem distinguishing projective knots. For example here we discuss an infinite family of pairs of knots which have identical associated virtual knots.

Consider the affine trefoil knot as shown in Figure 32. Notice that the virtual knot associated to this is the classical trefoil knot. Choose a non-affine unknot passing nearby this knot as in Figure 33. We may remove a small arc from the affine knot and the non-affine unknot and join the remaining parts of both of the knots. We will get a knot as shown

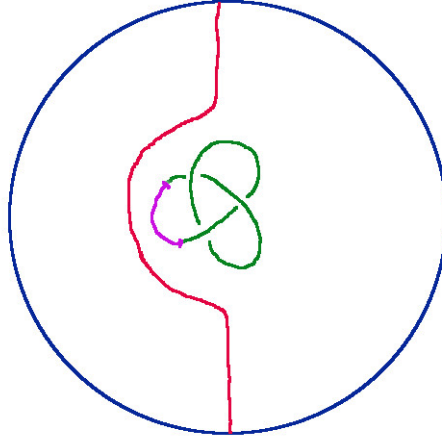


FIGURE 33. Affine trefoil knot and a non-affine un-knot

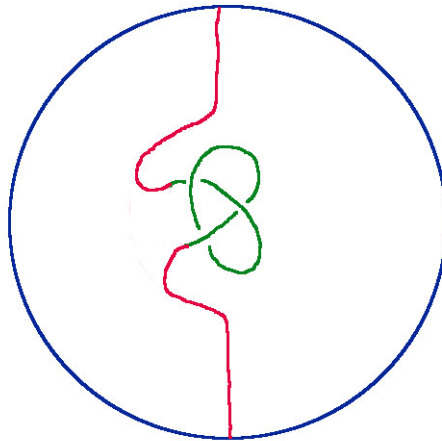


FIGURE 34. Non-affine trefoil knot

in Figure 34. This is a class-1 knot and hence distinct from the knot we started with. This process is called “projectivization” in [16]. Notice that the virtual knot associated to both the projectivized trefoil knot and the affine trefoil knot, by our mapping P is the classical trefoil knot.

An interesting example is the case of the Figure-8 knot. If we projectivize the affine Figure-8 knot on two different regions, we will get two diagrams as shown in Figure 35. It is not clear to the authors whether these two diagrams represent the same knot. Notice that the virtual knot associated to both of these knots, is exactly the classical Figure-8 knot. Hence our method of associating a virtual knot does not help in the problem of distinguishing these knots as projective knots. Thus none of the virtual knot invariants or the Jones polynomial of Drobotukhina [17] will help us here.

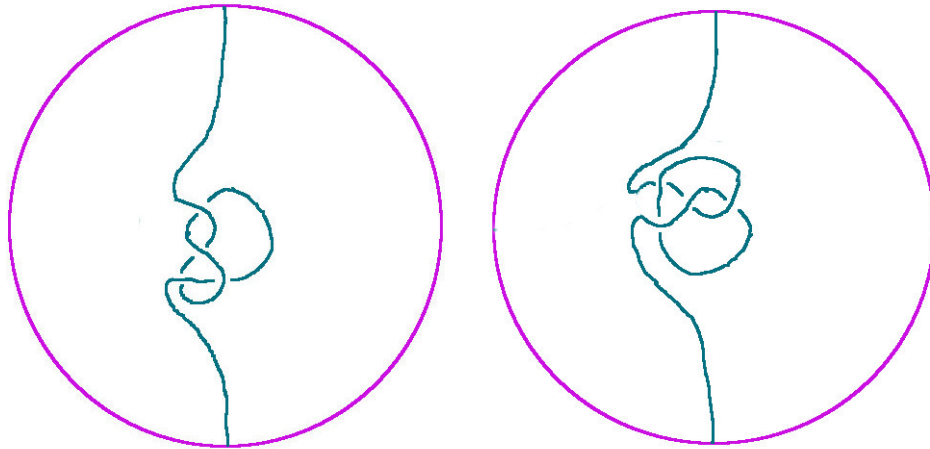


FIGURE 35. Diagrams of two projectivizations of the Figure-8 knot

$$\begin{array}{c}
 \begin{array}{ccc}
 & b & \\
 & \diagdown & \diagup \\
 c & & a \\
 & \diagup & \diagdown \\
 & d &
 \end{array}
 & = & X[a, b, c, d] \\
 \\
 \begin{array}{ccc}
 & & y \\
 & \curvearrowright & \\
 x & &
 \end{array}
 & = & \text{del}[x, y]
 \end{array}$$

FIGURE 36. Conversion formula to the code.

8. APPENDIX: BRACKET POLYNOMIAL OF THE KNOT IN FIGURE 27

We may index the arcs of the diagram as in Figure 37. The *Mathematica* code for computing the bracket is shown in Figure below. The conversion rules are given in Figure 36.

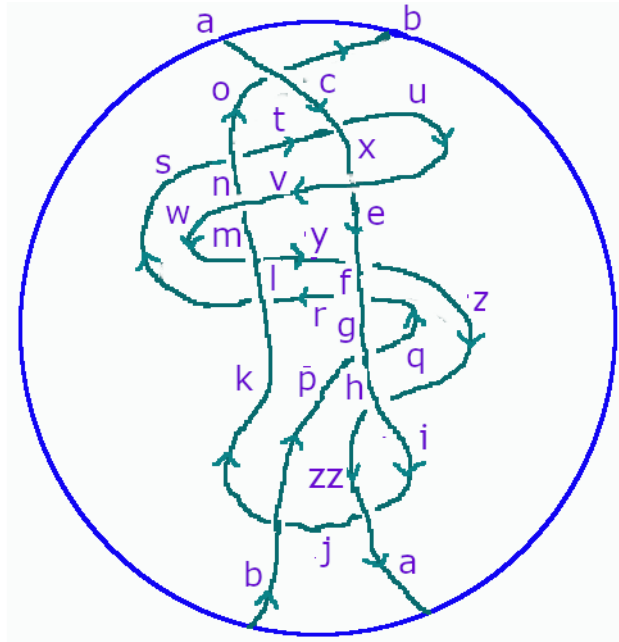


FIGURE 37. Indexing the arcs of the ribbon knot in Figure 27 to calculate bracket polynomial.

In[101]:=

```
rule1 = {X[a_, b_, c_, d_] => A del[a d] × del[b c] +
          B del[a b] × del[c d]};
rule2 = {del[a_b_] × del[b_c_] => del[a c]};
rule3 = {(del[_])^2 => dd, del[_^2] => dd};
RawBracket[t_] := Simplify[(t /. rule1 // Expand) /. rule2 /. rule3]
rule4 = {B => 1/A, dd => -A^2 - 1/A^2};
B[t_] := Simplify[RawBracket[t] / dd /. rule4]
BB[t_] := Simplify[RawBracket[t] /. rule4]
```

In[128]:=

```

ClearAll[a, b, c, d, e, f, g, h, i, j, k, l, m, n, o, p, q, r, s, t, u, v, w, x, y, z]
Ribbon = X[c, b, a, o] × X[c, t, x, u] × X[u, x, v, e] ×
  X[n, t, o, s] × X[v, n, w, m] × X[k, r, l, s] × X[m, w, l, y] × X[e, y, f, z] ×
  X[f, r, g, q] × X[g, p, h, q] × X[i, z, h, zz] × X[p, k, b, j] × X[zz, j, a, i]
Expand[B[Ribbon]]
Expand[(-A^(-3)) B[Ribbon]]

```

Out[129]=

```

X[c, b, a, o] × X[c, t, x, u] × X[e, y, f, z] × X[f, r, g, q] ×
  X[g, p, h, q] × X[i, z, h, zz] × X[k, r, l, s] × X[m, w, l, y] ×
  X[n, t, o, s] × X[p, k, b, j] × X[u, x, v, e] × X[v, n, w, m] × X[zz, j, a, i]

```

Out[130]=

$$-\frac{1}{A^{15}} - \frac{1}{A^{13}} + \frac{1}{A^{11}} + \frac{2}{A^9} - \frac{2}{A^5} + \frac{2}{A} + A - 2A^3 - A^5$$

Out[131]=

$$2 + \frac{1}{A^{18}} + \frac{1}{A^{16}} - \frac{1}{A^{14}} - \frac{2}{A^{12}} + \frac{2}{A^8} - \frac{2}{A^4} - \frac{1}{A^2} + A^2$$

(Not all divisible by 4 implies the knot is virtual or as projective not affine **)**

REFERENCES

- [1] J. S. Carter, S. Kamada and M. Saito: *Stable equivalences of knots on surfaces and virtual knot cobordisms*, Knots 2000 Korea, Vol. 1, (Yongpyong), *JKTR* **11** (2002) No. 3, 311-322.
- [2] Dye, Heather A.; Kaestner, Aaron; Kauffman, Louis H.: *Khovanov homology, Lee homology and a Rasmussen invariant for virtual knots*, J. Knot Theory Ramifications **26** (2017), no. 3, 1741001, 57 pages.
- [3] Gabrovšek, Boštjan. “The categorification of the Kauffman skein module of $\mathbb{R}P^3$ ” Bulletin of the Australian Mathematical Society **88**, no. 3 (2013): 407-422
- [4] Mikhail Goussarov, Michael Polyak and Oleg Viro: Finite type invariants of classical and virtual knots, math.GT/9810073.
- [5] L.H. Kauffman: *State Models and the Jones Polynomial*, *Topology* **26** (1987), 395–407.
- [6] L. H. Kauffman: *Knots and Physics*, Fourth edition. Series on Knots and Everything, 53. World Scientific Publishing Co. Pte. Ltd., Hackensack, NJ, 2013. xviii+846 pp. ISBN: 978-981-4383-01-1.
- [7] L. H. Kauffman: *Introduction to virtual knot theory*. Journal of Knot Theory and Its Ramifications **21**, no. 13 (2012): 1240007.
- [8] L. H. Kauffman: *Virtual Knot Theory*, *European J. Comb.* **20** (1999), 663-690.
- [9] L. H. Kauffman: *A Survey of Virtual Knot Theory*, Proceedings of Knots in Hellas '98, World Sci. Pub. 2000, 143-202.
- [10] L. H. Kauffman: *Detecting Virtual Knots*, Atti. Sem. Mat. Fis. Univ. Modena Supplemento al Vol. **II**, 241-282 (2001).

- [11] L. H. Kauffman: Knot diagrammatics, Handbook of Knot Theory, edited by Menasco and Thistlethwaite, 233–318, Elsevier B. V., Amsterdam, 2005.math.GN/0410329.
- [12] N. Kamada and S. Kamada: *Abstract link diagrams and virtual knots*, *JKTR* **9** (2000), No. 1, 93-106.
- [13] Lickorish, WB Raymond. “A representation of orientable combinatorial 3-manifolds.” *Annals of Mathematics* 76, no. 3 (1962): 531-540.
- [14] C. Manolescu and M. Willis: *A Rasmussen Invariant for links in RP^3* , arXiv:2301.09764v1.
- [15] V. O. Manturov: *Khovanov’s homology for virtual knots with arbitrary coefficients*, (Russian) *Izv. Ross. Akad. Nauk Ser. Mat.* 71 (2007), no. 5, 111–148; translation in *Izv. Math.* 71 (2007), no. 5, 967D999. *J. Knot Theory Ramifications* 16 (2007), no. 3, 345D377. math.GT/0601152.
- [16] Rama Mishra, Visakh Narayanan: *Geometry of knots in real projective 3-space*, *Journal of Knot Theory and Its Ramifications* 32, no. 10 (2023): 2350068.
- [17] Yu. V. Drobotukhina: *An analogue of the Jones polynomial for links in RP^3 and a generalization of the Kauffman-Murasugi theorem.*, *Algebra i analiz* 2, no. 3 (1990): 171-191.
- [18] Eliahou, S., Kauffman, L. H., & Thistlethwaite, M. B.: *Infinite families of links with trivial Jones polynomial*, *Topology*, 42(1), 155-169 (2003).

Louis H. Kauffman
 Department of Mathematics, Statistics
 and Computer Science (m/c 249)
 851 South Morgan Street
 University of Illinois at Chicago
 Chicago, Illinois 60607-7045
 <kauffman@uic.edu>,

Rama Mishra
 Indian Institute of Science Education and Research, Pune, India
 <r.mishra@iiserpune.ac.in>
 and

Visakh Narayanan
 Indian Institute of Science Education and Research, Mohali, India
 <visakh@iisermohali.ac.in>